Sustainable and Multifunctional Composites of Graphene-Based Natural Jute Fibers

Nazmul Karim,* Forkan Sarker, Shaila Afroj, Minglonghai Zhang, Prasad Potluri, and Kostya S. Novoselov

Smart and sustainable natural fiber-based composites are of great interest due to their biodegradability, recyclability, and environmental benefits over synthetic fiber composites. In addition, the environmental impact of plastics and synthetic fibers are widespread and substantial, as they can stay in the environment for hundreds of years and contribute significantly to global carbon emissions. Natural fibers such as jute can potentially replace synthetic fibers to manufacture environmentally sustainable, biodegradable, and lightweight composites with improved properties, good thermal and acoustic insulation, and a smaller carbon footprint. However, natural jute fiber-based composites suffer not only from poor mechanical properties but also being inherently electrically insulating, which limits their applications as multifunctional composites. Here multi-functional and environmentally sustainable smart composites of graphene-based natural jute fibers with excellent tensile and interfacial properties are reported. The reduced graphene oxide-based natural jute fiber enhance the Young's modulus of the composites by ≈450%, and tensile strength by ≈183% after physical and chemical treatment. Such high-performance composites can also be used as multifunctional smart composites, as demonstrated by effective electro-magnetic interference shielding performance. This may lead to manufacturing of next generation smart, strong, and sustainable natural fiber composites for high performance engineering applications without conferring environmental problems.

1. Introduction

In recent years, sustainable and biodegradable natural fibers[1–3] have attracted significant interests due to growing environmental concerns with plastics and synthetic fibers such as glass and carbon. The environmental impact of plastics and synthetic fibers are widespread and substantial (Table S1, Supporting Information). For example, plastics can hang around the environment for ≈450 years[4] and contribute to ≈15% of global carbon emissions;[5] glass and carbon fibers have an impact of ≈2.5 and ≈29.4 tonnes CO_2-eq per tonne of fiber production, respectively.[6] Therefore, there is a pressing need for sustainable, biodegradable, and lightweight materials for structural composite applications, that would offer unprecedented combinations of stiffness, strength and toughness at low density, and could be manufactured at high volume and low cost.[7] Natural fiber composites have shown great potential to replace synthetic fiber-based composites, due to their higher specific mechanical properties, good thermal and acoustic insulation, and smaller carbon foot print (Table S2, Supporting Information).[8] Jute, known as the "golden fiber" which is extracted from the bark of the white jute plant (*Corchorus capsularis*), and is a 100% bio-degradable, recyclable, and environmentally friendly natural fiber. It is also the second mostly produced natural fiber in the world after cotton, mainly in developing countries such as Bangladesh, China, and India, and at least ≈50% cheaper than flax and other similar natural fibers.[9]

Dr. N. Karim, Dr. S. Afroj
Centre for Fine Print Research
The University of West of England
Bristol BS3 2JT, UK
E-mail: nazmul.karim@uwe.ac.uk

Dr. N. Karim, Dr. S. Afroj, Prof. K. S. Novoselov
The National Graphene Institute (NGI)
The University of Manchester
Booth Street East, Manchester M13 9PL, UK

Dr. F. Sarker
Department of Textiles Engineering
Dhaka University of Engineering and Technology
Gazipur, Bangladesh

Dr. F. Sarker, Prof. P. Potluri
The Department of Materials
The University of Manchester
Oxford Road, Manchester M13 9PL, UK

M. Zhang
Institute of Textile and Clothing
The Hong Kong Polytechnic University
Hong Kong, China

Prof. K. S. Novoselov
Department of Materials Science and Engineering
National University of Singapore
9 Engineering Drive 1, Singapore 117575, Singapore

Prof. K. S. Novoselov
Chongqing 2D Materials Institute
Liangjiang New Area, Chongqing 400714, China

The ORCID identification number(s) for the author(s) of this article can be found under https://doi.org/10.1002/adsu.202000228.

**ADVANCED
SCIENCE NEWS**

www.advancedsciencenews.com

**ADVANCED
SUSTAINABLE
SYSTEMS**

www.advsustainsys.com

However, jute fiber reinforced composites suffer from lower mechanical and poor interfacial properties, due to the lower crystallinity and hydrophilicity introduced via larger amount (≈20–50 wt%) of non-cellulosic materials in their structure.[10,11] Moreover, jute fibers are inherently electrically insulating, which limits their application as multifunctional composites, when electrical conductivity is required.

"Smart" multifunctional composites are very popular at the moment, due to their ability to reversibly respond to one or more environmental stimuli such as chemical, electrical, light, temperature, and mechanical. Traditionally, smart composites are based on metals, polymers, and carbon-based nanomaterials.[12–14] However, metals and polymer-based composites suffer from oxidation and poor mechanical properties, respectively. In contrast, carbon nanomaterials have potential for "smart" multifunctional composites, as they are usually cost-effective, stable, mechanically strong and flexible, and electrically and thermally conductive.[15] Carbon nanotubes (CNT) have been investigated extensively as "smart" materials,[16] however the process of CNT synthesis is expensive and complicated. Conversely, graphene demonstrates multifunctional properties such as large specific surface areas, high electrical and thermal conductivity, and excellent mechanical properties.[17–19] In addition, graphene derivatives such as reduced graphene oxide (rGO) can not only be produced in a scalable and cost-effective way, but also be grafted into natural fiber via suitable bondings. Thus, graphene-based materials are ideal candidate for making "smart" natural fiber-reinforced composites with capability of electromagnetic interference (EMI) shielding, structural health monitoring (SHM), de-icing, and energy storage. In our previous studies,[20,21] graphene materials such as graphene oxide (GO) and graphene flakes (G) were deposited on jute fibers which improved tensile and interfacial properties significantly. However, GO is electrically insulating and not suitable for "smart" composite applications; whereas G flakes are almost without any oxygen-containing functional groups, and suffer from poor interfacial properties due to the absence of a suitable bonding with natural fibers. Thus, rGO could be an ideal material for making high performance, multifunctional, and environmentally sustainable natural fiber composites. It could provide excellent mechanical properties due to specific interaction between residual oxygen functional groups of rGO and that of natural fibers,[22,23] as well as imparting electrical and thermal properties required to make next generation "smart" composites.

Here, we report multi-functional and environmentally sustainable smart composites of rGO-based natural jute fibers with excellent tensile and interfacial properties. We used scalable synthesis of rGO in a water-based and biocompatible dispersion, and a facile coating technique to produce graphene-coated unidirectional jute fiber preforms with new fiber architecture, before jute/epoxy composites were manufactured via a simple vacuum resin infusion process. Graphene-based single jute fibers were characterized, tested, and analyzed to investigate tensile and interfacial properties. The improvement in longitudinal and transverse mechanical properties of composites, and their fracture surface was tested and analyzed. A potential application of multifunctional graphene-based natural fiber composites as EMI device is demonstrated. Finally, the environmental impact, sustainability, and mechanical properties of our graphene-based natural jute fiber-reinforced composites were analyzed and compared with that of synthetic fiber-reinforced composites.

2. Results and Discussion

2.1. Scalable Production of Graphene-Based Natural Jute Fibers

rGO is a graphene derivative, composed of perfect graphene sheet with small number of hydroxyl epoxy and other groups attached to it. As a result, it demonstrates similar mechanical and electronic properties to pristine graphene. Though numerous efforts have been made to produce pristine graphene-like materials via reduction of GO to rGO, only partial restoration of graphene-like structure is possible with residual functional groups and structural defects.[24] However such residual functional groups are perfect for creating suitable bonding with that of natural fibers to enable durable and uniform rGO coatings. Moreover, rGO could be produced in a scalable quantity due to simple and cheap production process of its precursor: GO. Here, a previously reported process to prepare GO via a modified Hummers method was used, with subsequent reduction to rGO via an in situ-chemical reduction process of GO.[23,25,26] The average flake thickness and size of as prepared rGO is found to be ≈2.26 nm and ≈4.86 µm, respectively, confirming the presence of single to few layers of graphene flakes in the dispersion. Raman spectra of rGO show the shifting of characteristics D and G peaks toward lower wave numbers: ≈1327.4 cm^{-1} (D) and ≈1596.82 cm^{-1} (G), which is due to the recovery of hexagonal symmetry of the lattice. The intensity ratio of the D and G band (I_D/I_G) is also increased from ≈0.98 (GO) to ≈1.73 (rGO).

Before rGO coating, jute fibers were cleaned, and pre-treated with heat and alkali (NaOH) as per the previous study.[20] Surface pre-treated jute fibers (HA0.5) were then coated with rGO using a simple dip-coating technique and oven dried at 80 °C for 30 min, **Figure 1**a. XPS analysis was used to characterize surface functionalities of untreated and rGO-coated jute fibers, Figure 1b–d. The wide scan XPS spectra shows that the C/O ratio of jute fibers decreases from ≈5.5 to ≈3.8 after coating with GO, due to the presence of oxygen containing functional groups in GO.[27,28] After rGO coating, C/O ratio increased to ≈7.1, due to the partial restoration of graphene structures, Figure 1b. The high resolution C1s X-ray photoelectron spectroscopy (XPS) spectrum of untreated jute fibers confirms the presence of three main components: C−C bond (≈284.5 eV) in cellulosic structure, C−O−C groups (hydroxyl and epoxy, ≈286.5 eV) and C=O groups (carbonyl, ≈288.3 eV), Figure 1c.[24] After coating with rGO, the peaks associated with the oxygen functional groups significantly diminished with small amounts of residual oxygen functional groups left as evident from the peak around 287.5 eV, Figure 1d.[23,25,26]

Figure S1a, Supporting information shows SEM images of a smooth and featureless untreated jute fiber surface, which may be due to the presence of a cementing layer that is composed of waxes, fats, lignin, pectin, and hemicelluloses.[29] The coating of rGO results in a more uniform, highly individualized, and evenly coated fiber surface with only a few flakes present on the surface (Figure S1d, Supporting Information), which may

**ADVANCED
SCIENCE NEWS**

www.advancedsciencenews.com

**ADVANCED
SUSTAINABLE
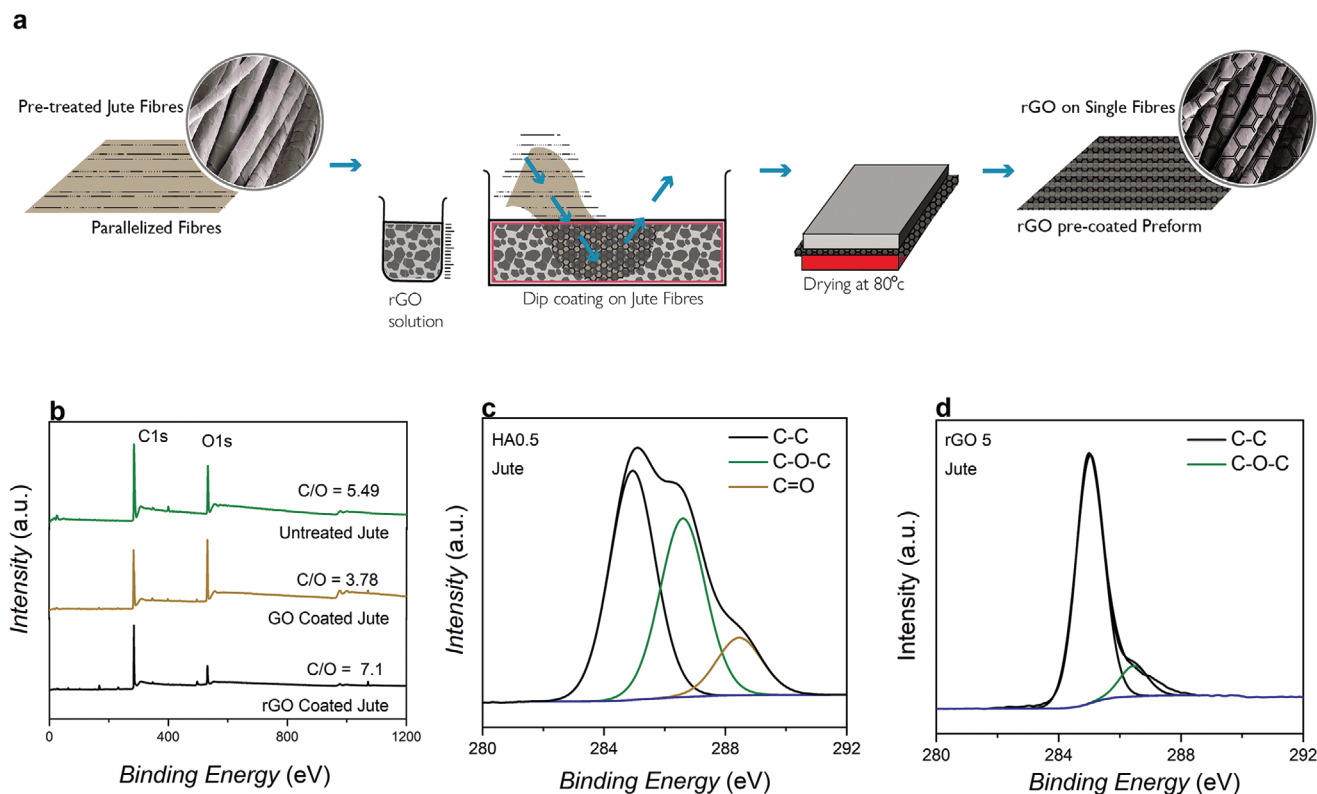SYSTEMS**

www.advsustainsys.com

Figure 1. a) Schematic diagram showing rGO coating process on jute fibers and the preparation of rGO-coated jute fibers preforms, b) wide scan XPS spectrum of graphite, G flakes, GO, and rGO, c) high resolution C(1s) XPS spectrum of untreated jute fiber, and d) high resolution C(1s) XPS spectrum of rGO-coated jute fiber.

be due to chemical bonding provided by the functional groups of rGO.[22] The diameter of untreated jute fibers is found to be ≈55 ± 12 µm, which is reduced to ≈43 ± 8 µm (Figure S1c, Supporting Information) after heat and alkali treatment, which may be due to the removal of hemicellulose, pectin, and lignin. The diameter of rGO-coated jute fibers (HA rGO5) reduced further by ≈34.5% to ≈36 ± 16 µm (Figures S2b and S4a, Supporting Information), unlike the previously reported study where coating with GO and G flakes increase the diameter of HA0.5 jute fibers slightly.[20] Fourier transform infrared spectroscopy (FTIR) analysis confirms the removal of hemicellulose and lignin after rGO coatings. Moreover, a characteristic peak is identified at ≈2400 cm⁻¹ band for rGO-coated fiber indicates the conjugated C=C bonding between the functional group of rGO and jute fiber (Figure S3a, Supporting Information). TGA analysis shows that rGO coating improves the thermal stability of HA0.5 jute fibers, which may be due to the formation of a carbonaceous coating of graphene like materials on the fiber surface, which delays the degradation and improves thermal stability of the fiber. This was confirmed by the increase of residue% from ≈17% for untreated fibers (UT) to ≈36% for rGO-coated jute fiber (Figure S3b, Supporting Information).

2.2. Single Fiber Tests: Tensile and Interfacial Properties

First, a single fiber test was used to get an insight into the effect of tensile and interfacial properties of individual rGO-coated jute fiber on the behavior of final jute fiber reinforced composites. Static and dynamic single fiber tests (**Figure 2**a) are more difficult to conduct due to the small diameter of the fiber, which imposes great challenges in fiber handling and clamping due to the slippage. We used 50 single fibers for each test and then plotted average results from those 50 samples in Figure 2b–d and Table S3, Supporting Information. The tensile modulus and strength of UT are found to be ≈30 GPa and ≈295 MPa, respectively, which increase slightly after heat and alkali treatment (HA0.5) and are similar to those reported in our previous study.[20] After rGO5 (5 wt%) coatings, the Young's modulus of jute fiber increases from ≈30 to ≈78 GPa, and the tensile strength from ≈295 to ≈814 MPa, which are ≈160% and ≈174.5% increment compared to that of UT. This is the highest tensile properties obtained so far with alkali treatment and nanosurface engineering of jute fibers to the best of our knowledge. As expected, the tensile properties of jute fibers improve with the increase in rGO concentrations (0.5–5 wt%), Figure 2b,c. Although fiber breaking strain and breaking force reduced initially after alkali treatment, they are increased by 38% and 71%, respectively, after rGO5 coating on jute fibers, Figure 2d and Table S3, Supporting Information. In addition, the area under the stress–strain curve provides the higher extension, which demonstrates excellent flexibility and higher toughness against fracture of rGO5-coated jute fibers under tensile stress. (Figure S4b, Supporting Information).

The excellent tensile properties with rGO coatings could be explained by Faber and Evan's crack deflection theory.[30] The
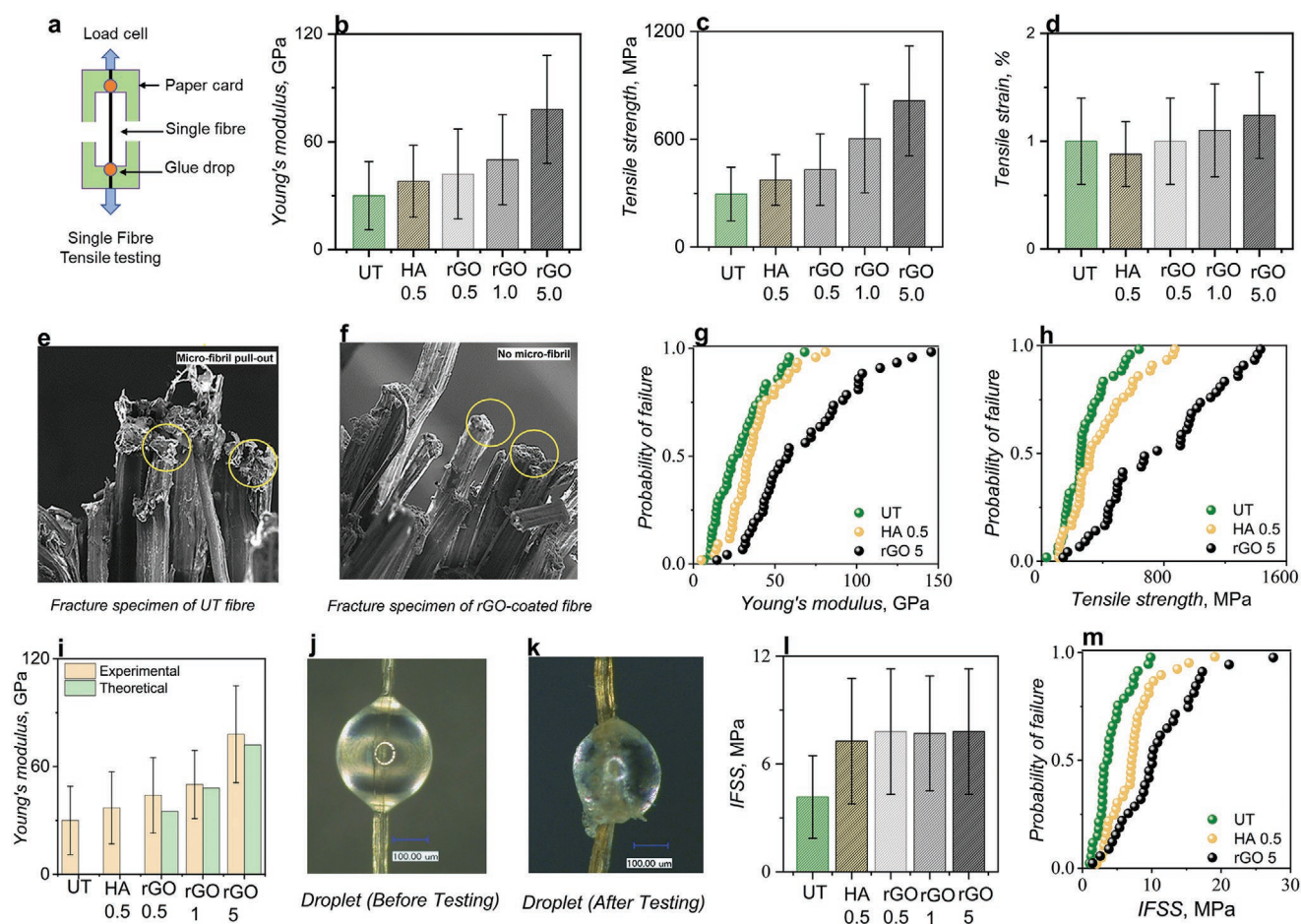
Figure 2. Single fiber tensile and interfacial properties. a) Sample preparation for single fiber test, b) Young's modulus, c) tensile strength and d) tensile strain% of untreated, HA0.5, and rGO-coated jute fibers. e) SEM images of the fracture specimen after single fiber tensile test without any treatment (X250) and f) SEM images of the fracture specimen after tensile test of single jute fiber after rGO coating (X250). g) Young's modulus and h) tensile strength data fitted to a two-parameter Weibull probability distribution as function of surface treatment. i) Comparative analysis of theoretical and experimental Young's modulus of untreated and graphene-based jute fibers. Optical images of microdroplets of rGO-coated fiber: j) Before testing and k) after testing. l) Interfacial shear strength (IFSS) of untreated, HA0.5, and rGO-coated jute fibers, m) Interfacial shear strength (IFSS) data fitted to a two-parameter Weibull probability distribution as function of surface treatment.

rGO flakes could possibly increase the crack area by deflecting any advancing crack and thus reducing the stress generated at their tip. This is because the rate of effective crack deflection depends on the orientation of platelet particles perpendicular to the crack growth. Additionally, in a neat graphene system three types of dominant interactions exist between graphene sheets: van der Waals interaction, hydrogen bonds, and coordinative cross-linking. After the chemical reduction of GO, the van der Waals interaction along the decreasing interlayer space and the hydrogen bonds between residual oxygen functional groups are increased. As a result, the mechanical properties of coated fibers are enhanced.[31] Furthermore, the presence of PSS polymers in rGO dispersions, and partial reduction of GO might increase the stacking and slippage of the graphene sheets stacking and slip, which enhances the elongation and breaking force.[32] SEM of the rGO-coated jute shows highly individualized fibers, in Figure S1d, Supporting information. The pores on the fiber surface are filled with rGO flakes, which improve the uniformity in the network structure, resulting in

an enhancement of the stress transfer and the tensile strength of jute fibers. The fracture specimen after tensile test was also investigated, which shows uneven microfibrils fracture for untreated jute fibers due to stress concentration between the cellulosic microfibrils in the fiber, Figure 2e. However, when the fibers are coated with rGO5, a linear breakage of microfibrils is observed which is responsible for more loading capacity along the tensile deformation, Figure 2f.

A two-parameter (scale parameter, α and shape parameter, β) Weibull distribution was used (Equations (S1)–(S6) and Table S3, Supporting Information), where α predicts experimental results and β indicates the modulus of Weibull distribution known as Weibull modulus. Figure 2g,h shows that the distribution for both Young's modulus and tensile strength shifted significantly from the left to right side after fibers are treated with rGO. The untreated jute fibers provide a lower value of Weibull modulus ≈1.86 (Figure S6a,b, Supporting Information), which indicates higher scattering in the tensile properties of untreated jute fiber, due to the non-homogenous nature of the

**ADVANCED
SCIENCE NEWS**

www.advancedsciencenews.com

**ADVANCED
SUSTAINABLE
SYSTEMS**

www.advsustainsys.com

fiber. However, the Weibull modulus increases up to ≈2.46 after rGO grafting, which may be due to the better bonding between fibers and rGO as explained earlier. A well-established Halpin–Tsi model was also used to theoretically predict the reinforcing mechanism of rGO-coated jute fibers and calculate theoretical value of Young's modulus (Equations (S7)–(S11) and Table S4, Supporting information).[20] Figure 2i shows that the Young's modulus increases with the increase of rGO concentrations both in experimental and theoretical results. The predicted tensile modulus of graphene-coated fibers (rGO5) is slightly (≈5%) less than the experimental results, which is acceptable due to the wrinkled structure of graphene flakes rather than the rectangular shape, which was assumed in our theoretical calculation and detailed by Tian et al.[33] Figure 2j,k shows the optical images of microdroplets before and after a micro-bond test. The micro-bonding test of untreated jute fibers shows relatively lower interfacial shear strength, IFSS (≈4.16 MPa) for untreated jute fiber-epoxy micro-composites, which increases to ≈7.37 MPa after heat alkali treatment (HA0.5), Figure 2l. After coating with rGO5, IFSS increases slightly to ≈8.2 MPa, Figure 2l and Table S5, Supporting Information. Like tensile properties the Weibull distribution for IFSS shifted from the left to right, Figure 2m and Figure S6c, Supporting Information. Comparative study (Table S6, Supporting Information) confirms the effect of rGO on improving the IFSS value is better than other natural and synthetic fibers modified by traditional alkali and nanomaterials.

2.3. Ultra-Strong Composites of Graphene-Based Natural Jute Fibers

The untreated unidirectional jute fiber composites have relatively lower tensile properties: The Young's modulus of ≈10 GPa and tensile strength of ≈180 MPa is due to presence of excessive amount of non-cellulosic materials like hemicellulose and lignin, **Figure 3**a–c. We therefore developed new jute fiber architecture to remove those non-cellulosic materials, and to obtain Young's modulus of ≈27.6 GPa and tensile strength of ≈232 MPa (Table S7, Supporting Information). Such improvement could be explained by the individualization and compaction of fibers to increase the fiber volume fraction (V_f) (Equations (S12) and (S13), Supporting Information) and load-bearing capacity of the composites.[21] Further treatment with alkali and a hot press improves the fiber packing (Figure S7b, Supporting Information) and fiber-matrix interfacial adhesions. Our previous studies[20,21] reported that coatings of graphene materials (GO and G flakes) on surface pre-treated jute fibers could increase the surface wettability and roughness of the fiber; thus, enhance the interfacial and mechanical properties of the composites significantly. Similarly, we prepared unidirectional rGO-coated new jute fiber preform by combining physical and chemical treatment (NFHP), and then used those preforms to prepare fiber reinforced composites via a simple vacuum resin infusion process, Figure 3d.[21] The Young's modulus and tensile strength of as prepared composites increase significantly, from ≈27.6 to ≈55 GPa and ≈232 to ≈510 MPa with rGO5 (0.5 wt%) coated jute fibers. (Figure 3a–c; Table S7, Supporting Information). The combination of all physical and chemical

treatments together with rGO coating results in ≈450% and ≈183% improvement in the Young's modulus and tensile strength of the composites, which is the highest improvement in the tensile properties of any kind of natural fiber composites reported in the literature (**Table 1**). As per rule-of-mixture, such massive improvement in tensile properties of natural jute fiber composites may be due to the significant increment in fiber volume fraction (V_f) (Table S7, Supporting Information) after combined physical (individualization and compaction) and chemical (alkali and rGO) treatments. To better understand the effect of rGO coating on the IFSS at composite level, we carried out tensile testing in transverse direction of the composites, Figure 3e–g. As expected, the untreated fiber and fiber with new architecture shows relatively lower transverse tensile properties, due to the fiber impurities that caused poor interfacial adhesion between the fiber and matrix. After rGO coatings, transverse tensile properties of jute fiber composites improve almost ≈100% in comparison to that of untreated fiber. This may be due to the increased surface roughness and mechanical inter-locking between the fiber and matrix with rGO coating.

A stress–strain curve clearly shows uninterrupted stress development for rGO-coated jute fiber composites, which can be considered as a similar behavior to glass or carbon like monolithic reinforcing materials in composites, Figure 3h. We examine the fracture surface of the composites specimen after tensile test using a scanning electron microscope (SEM), Figure 3i,j. For the untreated jute fiber composite, the surface of the composites fails predominantly due to the weak interfacial bonding and the fiber pull-out, Figure 3i. The fracture surface of rGO-coated jute fiber composites shows an uneven scattered failure of fibers and also a strong inter-fibrillar connection between each individual jute fiber, Figure 3j and Figure S8a, Supporting Information. However, SEM images of fractured surfaces in traverse directions show a complete matrix failure (matrix debonding) from the fiber, which is the reflection of poor interfacial shear failure of the composites (Figure S8b, Supporting Information).[34] We then examined the cross section of coated jute fiber composites to study the packing order and porosity related issues of the composites. Natural fiber-based composites are always susceptible to producing different porosities[35] such as matrix porosity, impregnation porosity, and luminal porosity, due to inherent flaws and lower crystallinity.[36] In contrast, rGO-coated jute fibers composites show strong packing of fibers and no such porosity related issues (Figure S7b, Supporting Information).

2.4. Multifunctional Composites of Graphene-Based Natural Fibers

High performance, multi-functional, and bio-compatible composites are becoming increasingly attractive to composite manufacturers and material scientists, due to their ability to provide excellent mechanical, thermal, electrical, and opto-electrical properties.[37] Recently nanomaterials such as conductive polymers, metals, CNT, and other carbon-based materials have been investigated to make electrically and thermally conductive "Smart Composites" with improved mechanical properties for multifunctional applications such as SHM, EMI shielding, and
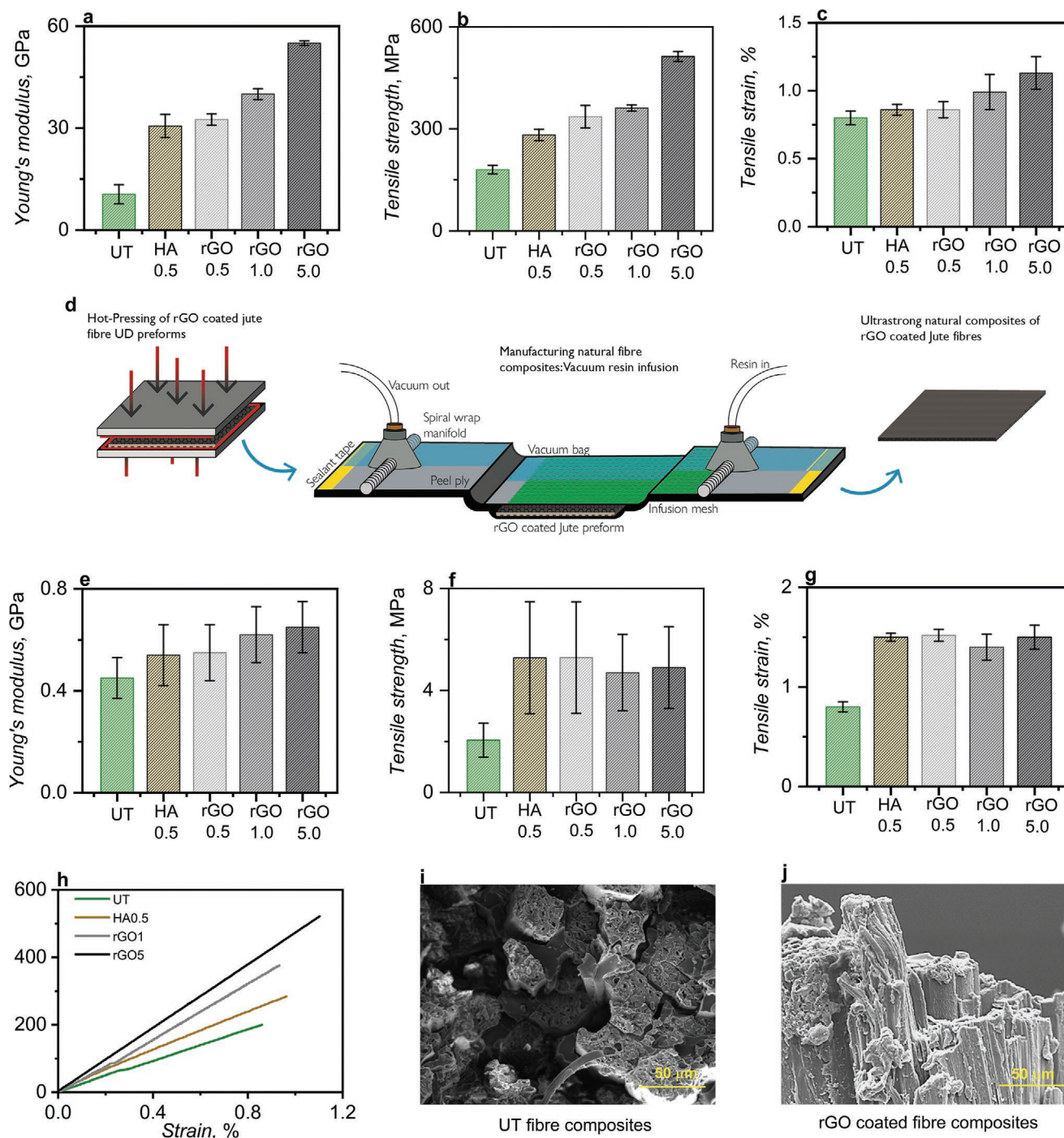
Figure 3. a) Young's modulus, b) tensile strength, and c) strain % of untreated, new fiber architecture, and different concentrations of rGO-coated jute fiber epoxy composites in longitudinal direction. d) Schematic of rGO-coated jute fiber reinforced composites manufacturing process, e) Young's modulus, f) tensile strength, and g) strain % of untreated, new fiber architecture, and different concentrations of rGO-coated jute fiber epoxy composites in transverse direction. h) Stress–strain curves of untreated, HA0.5 treated, rGO1, and rGO5 treated jute fiber reinforced composites. i) SEM image of the fracture surface of UT fiber reinforced composites, and j) SEM image on the fracture surface of rGO-coated composites in longitudinal direction.

joule heating.[13,38,39] The outstanding electrical, mechanical, and thermal properties, high surface area, and cost-effective production cost of graphene-based materials[17–19] made them perfect material for multi-functional "smart" composite application. Our multifunctional composites of graphene-based

natural fiber composites not only demonstrate excellent tensile properties but also demonstrate relatively high electrical and thermal conductivity. Thus, they could potentially be applied for smart composites applications with capabilities of EMI, SHM, de-icing, and energy storage. Here, we demonstrate potential

Table 1. Comparative tensile properties of graphene-coated jute fiber/epoxy composites with other surface-treated natural fiber composites in the literatures.

Fibers	V_f [%]	Young's modulus, GPa			Tensile strength, MPa			Ref.
		Before treatment	After treatment	Change [%]	Before treatment	After treatment	Change [%]	
Fiber scale								
Sisal (SNC)	–	–	–	–	512	451	+115.9	[46]
Oil Palm (CuNP)	–	4.1	4.5	+9.75	213	255	+18.6	[47]
Flax (Ti O$_2$ 2.35%)	–	30.5	32.5	+6.55	380	490.2	+29	[48]
Jute (GO 0.25%)	–	30	37	+23.3	295	394	+33.5	[20]
Jute (GO 0.5%)	–	30	44	+46.6	295	436	+47.7	[20]
Jute (GO 0.75%)	–	30	46	+53.3	295	501	+69.8	[20]
Jute (GO 1.0%)	–	30	48	+60	295	575	+94.9	[20]
Jute (rGO 1.0%)	–	30	50	+66.6	295	604	+104.7	This study
Jute (rGO 5.0%)	–	30	78	+160	295	814	+175.9	This study
Composites scale								
Ramie (CNT 0.7%)	–	6	7	+16.6	57	78	+36.8	[49]
Oil Palm (CuNP)	–	–	–	–	255	350	+37.25	[47]
Jute (GO 0.25%)	54	27.6	36.9	+33.6	232	295	+27.1	[21]
Jute (GO 0.5%)	54	27.6	42.8	+55	232	337	+45.2	[21]
Jute (GO 0.75%)	56	27.6	44.6	+61.5	232	379	+63.3	[21]
Jute (GO 1.0%)	55	27.6	37.8	+36.9	232	292	+25.8	[21]
Carbon (GO 5%)	48	45	55	+22.2	1750	2000	+14.28	[50]
Jute (rGO 1.0%)	59	27.6	40	+44.9	232	370	+59.4	This study
Jute (rGO 5.0%)	60	27.6	55	+99.2	232	510	+119.8	This study

– stands for information not given.

EMI shielding application of three composite samples comprised of five layers of UD jute fiber preforms (HA0.5 treated, rGO coated, and G flake coated).

EMI is perceived as new form of pollution due to increased use of electronics and instrumentation in commercial and industrial settings.[40] EMI could interact with biological systems and, at high intensities can potentially damage the human body's DNA structure.[41] The EMI shielding mechanism of natural fiber composites samples (**Figure 4**a) could be explained by a combination of the high conductivity, smaller thickness (which guarantees significant transmission through a single layer), and layered structure (which ensures multiple reflections) of rGO. At 8.2 GHz frequency, the shielding effectiveness (SE)% increases from ≈49.2% for HA0.5 treated jute fiber composites to ≈77.1% for natural composites of rGO-coated jute fibers, Figure 4b. As expected the highest SE% (≈92.9%) is obtained for composites of G flake-coated jute fibers (Figure 4b), due to higher conductivity of G-coated jute fibers. Similarly, absorption% increased with the increase of the electrical conductivity of the sample, Figure 4c. The shielding mechanism of graphene material-coated jute composites is the combination of reflection and absorption of EM waves. Once EM waves are absorbed into the graphene-coated composites, it undergoes internal reflection due to the porous fiber structure and the layered structure of graphene flakes; thus, this dissipates EMI waves and improves the SE.

2.5. Sustainability, Environmental Impacts, and Comparative Study

Millions of people, especially from developing countries are involved in natural fiber industries, and as such, fiber-based products are processed and manufactured in many small and large industries around the world. Thus, the economic impact of the consumption of natural fiber-based products has been quite significant. For example, Jute is the second most produced natural fiber in the world after cotton (≈3.63 million tonnes annually, **Figure 5**a), and at least ≈50% cheaper than flax and other similar natural fibers. The use of jute for various applications could boost the farming economies of developing countries such as Bangladesh and India, where it is mostly produced. Jute is extracted from the bark of the white jute plant (*C. capsularis*), and a 100% bio-degradable, recyclable, and environmentally friendly natural fiber. However, natural fibers lost its glaze with the introduction of cheaper and high-performance synthetic fibers such as polyester and nylon for textile applications, and glass and carbon fiber for composites applications.
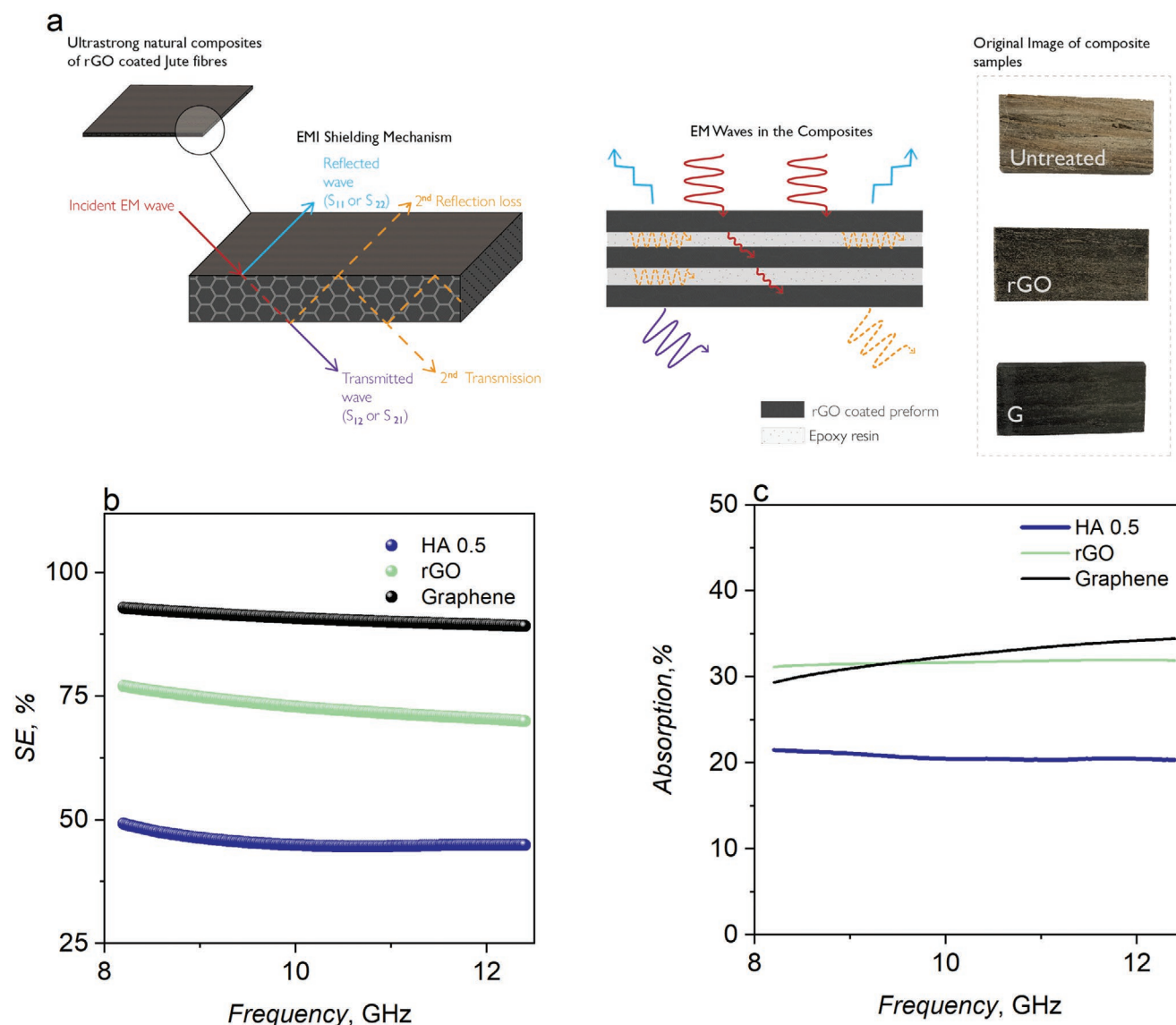
Figure 4. Multifunctional smart composites of graphene-based natural fiber. a) Schematic diagram of EMI shielding mechanism and graphene-based natural jute composites; b) shielding effectiveness% versus frequency and c) absorption% versus frequency.

Nevertheless, with growing environmental concerns with plastics and synthetic fibers, the use of natural fibers such as jute is on the rise again. Here, we compare the environmental impact, Materials Sustainability Index (MSI) score and properties of jute with their synthetic counterparts such as such as glass and carbon. It is worth mentioning that the composite preparation is similar for both synthetic and natural fiber reinforcements; we therefore analyses fiber performance for sustainability and environmental impact.

The production of glass and carbon fibers (≈1.14 and ≈0.15 million tonnes, respectively, in 2018) is increasing globally, due to the rise in the demand for high-performance and lightweight materials, Figure 5a–c. However, jute fibers are produced in larger quantities (≈3.63 million tonnes in 2018) with a rapidly increasing amount in recent years, and have always been the most dominant bast fiber, Figure 5d. The environmental impact of fiber production varies between their types. For example,

natural fibers consume less energy but more water during their production process than synthetic fibers.[42] The most pressing environmental impact with natural fiber production is the water usage during their cultivation. About 3% of global irrigation (≈44 trillion liters annually) water is used for textile fiber productions.[43] Indeed, jute has a higher water foot-print (0.08 m^3 kg^{-1} fiber) as per the water scarcity weighting than that of carbon (0.03 m^3 kg^{-1} fiber) and glass fibers (0.01 m^3 kg^{-1} fiber), Figure 5a–c. However, the energy consumption for jute fiber production (≈9.6 MJ kg^{-1} fiber) is ≈6 times and ≈30 times lower than that of glass (≈54.7 MJ kg^{-1}) and carbon (≈286 MJ kg^{-1}) fibers, respectively. Such higher energy consumption with synthetic fiber production is associated with their production process and higher manufacturing temperature for glass (1400–1500 °C) and carbon (≈1000 °C). As a result, the carbon footprint with synthetic fibers is significantly higher. For example, virgin carbon and glass fiber emits ≈29.4 and ≈2.5 tonne
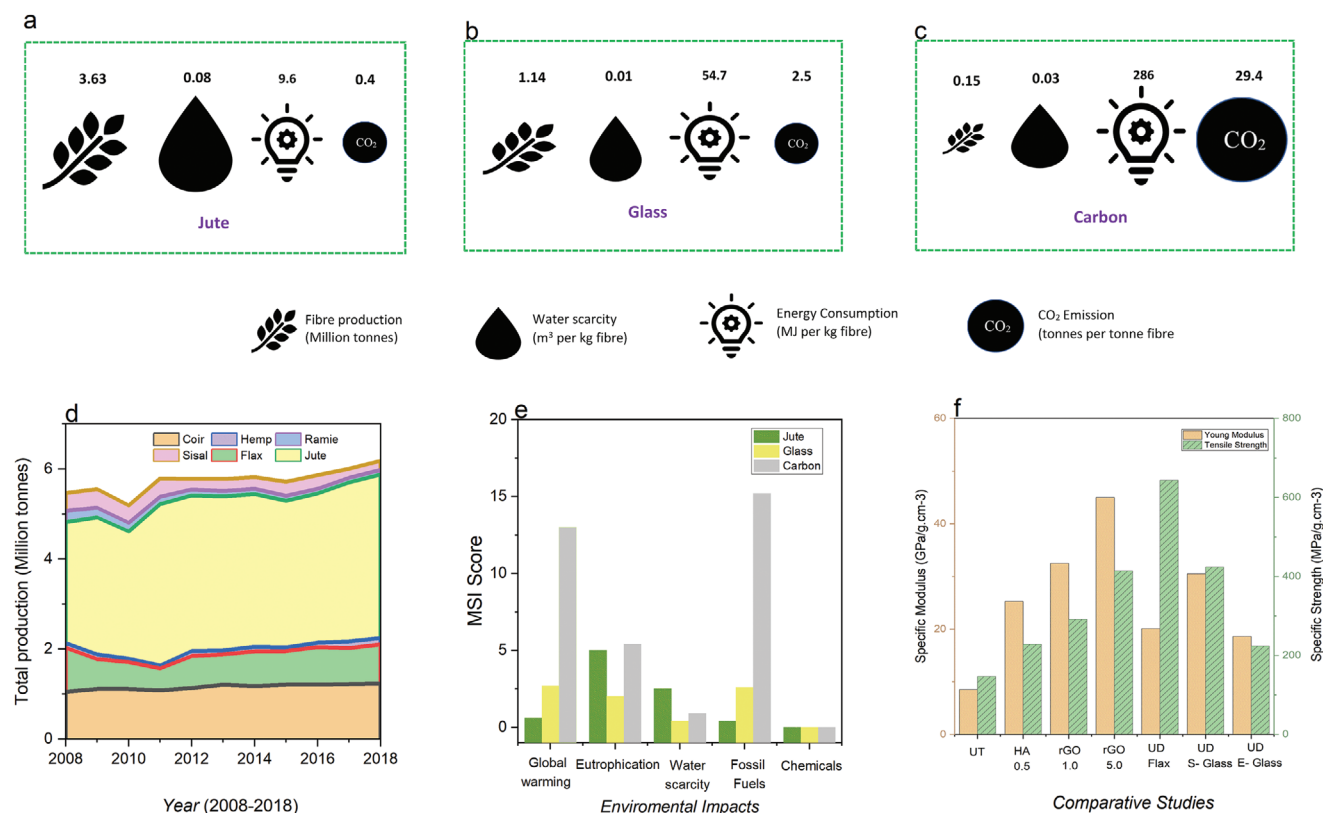
ADVANCED
SCIENCE NEWS
www.advancedsciencenews.com

ADVANCED
SUSTAINABLE
SYSTEMS
www.advsustainsys.com

Figure 5. Environmental sustainability, impacts, and comparative study. Fiber production, energy consumptions, water scarcity, and carbon emissions for a) jute, b) glass fiber, and c) carbon fiber; d) total bast fiber production globally from 2008 to 2018; e) Materials Sustainability Index (MSI) score for jute, glass, and carbon fiber and f) comparative specific properties of jute, flax, and glass fiber composites.

CO_2 for per tonne fiber production. In contrast, plant fibers such as jute act as a carbon sink by sequestering atmospheric carbon.[44] For example, one tonne of dry jute fiber could absorb ≈ 2.4 tonnes of CO_2. We also compare cradle-to-gate Higgs MSI score from the life cycle assessment to understand and quantify the sustainability impacts of jute, carbon, and glass fibers.[45] Carbon and glass fibers contribute toward global warming and fossil fuel consumption significantly higher than jute. However, jute fiber contribution to water scarcity is substantial, and its eutrophication is comparable to that of carbon fiber. Nevertheless, the replacement of synthetic fibers with natural plant-based jute for multi-functional composite applications could potentially provide sustainable and environmentally friendly composites; thus, reduces the greenhouse-gases impact with fiber reinforce composites significantly.

We then compare specific properties of untreated and treated jute fiber composites with that of flax, E-glass, and S-glass fiber composites Figure 5f. The specific Young's modulus of untreated jute fiber composites is found to be ≈ 8.7 GPa g^{-1} cm^{-3}, which increases to ≈ 42.3 GPa g^{-1} cm^{-3} for composites with HA-treated and rGO-coated fibers, Figure 5f. Thus, the Young's modulus of newly developed rGO5.0 coated jute fiber composites is $\approx 139\%$ and $\approx 79\%$ higher than that of E (≈ 17.7 GPa g^{-1} cm^{-3}) and S (≈ 23.6 GPa g^{-1} cm^{-3}) glass fibers, respectively. The specific strength of rGO-coated jute composites is found to be similar to that of E-glass fibers. Table 1 shows a comparison of rGO-coated jute fiber and their composites with other natural

fiber and their composites modified with nanomaterials, as reported in the literature. rGO-coated jute fibers show significantly higher Young's modulus of ≈ 78 GPa and tensile strength of ≈ 814 MPa, which is the highest reported value of mechanical properties based on natural fiber modified with nanomaterials. In order to check the suitability of our newly developed rGO-coated jute fiber/epoxy composite in high-performance applications where mainly glass and carbon fiber are used, we compare its tensile properties with both S-glass and E-glass fiber composites (Table S7, Supporting Information). In addition, Young's modulus of rGO-coated jute fiber/epoxy composite is found to be ≈ 55 GPa, which is $\approx 18\%$ and $\approx 40\%$ higher than that of S-glass (≈ 33.5 GPa) and E-glass (≈ 45.1 GPa) fiber/epoxy composites, respectively. The value of Young's modulus of rGO-coated jute fiber composites is even similar to that of GO-coated carbon fiber composites (≈ 55 GPa) as reported in the literature (Table 1). Thus, newly developed rGO-coated jute fiber composites cannot only be used as a replacement for glass for specific property-driven applications but also in stiffness-driven high-performance engineered structure applications.

3. Conclusion

In this study, we report the formation of multi-functional and environmentally sustainable smart composites of rGO-based natural jute fibers with excellent tensile and interfacial

**ADVANCED
SCIENCE NEWS**

www.advancedsciencenews.com

**ADVANCED
SUSTAINABLE
SYSTEMS**

www.advsustainsys.com

properties. Morphological and micro-structural investigations reveal that rGO is uniformly coated onto jute fiber surface. Thus, it shows a remarkable improvement in fiber and composite mechanical properties, as well as electro-magnetic properties of the composites, possibly due to the formation of suitable bonding between the residual oxygen functional groups of rGO and the hydroxyl groups of jute fibers. Therefore, smart, strong, and sustainable rGO-based jute fiber composites offer a great opportunity to replace its synthetic counterparts for high-performance engineered application, with an objective to develop next generation environmentally sustainable composite.

4. Experimental Section

Materials: Field retted "Tossa white Jute" fiber was collected from Bangladesh, cultivated in the northeast of Dhaka capital. Generally, the fiber cultivation starts from summer and finishes at the end of rainy season. The raw fiber bundles are commonly known as raw jute sliver collected after dew retting under the water of a pond or a river where there is continuous flow of water (Figure S9a,b, Supporting Information). The collected raw sliver contains ≈98–99% of technical fiber bundles and the rest of them are shives (the remainder of cortical tissues and impurities). Raw jute sliver has an average length of ≈2.9 m and diameter of ≈0.06 mm, respectively. Sodium hydroxide (NaOH) was purchased as pellets from a commercial supplier, Fisher Scientific, UK. Graphexel Limited, UK kindly supplied the natural flake graphite. The average lateral size of the flake was 50 mm. Sodium deoxycholate powder, potassium permanganate (KMnO$_4$), sulfuric acid (H$_2$SO$_4$, ≈99%), ammonia, poly(vinyl alcohol), poly(sodium 4-styrenesulfonate), sodium hydrosulfite, and hydrogen peroxide (H$_2$O$_2$, ≈30%) were purchased from Sigma Aldrich, UK. EPI-REZTM epoxy compatible water borne sizing (product no 7520-W-250) was purchased from Hexion, UK. S and E-glass were purchased from AGY, USA. A room temperature cured epoxy EL2 laminating resin and AT30 slow hardener were purchased from Easy Composites, UK. AT30 is cycloaliphatic amine-based mixture which forms a co-polymer with the expoxy resin to enable efficient curing.

Synthesis of Graphene Oxide and Reduced Graphene Oxide: GO was prepared using a modified Hummers method as described elsewhere.[5] 80 mg GO was added to 160 mL deionized water (DI), and left for at least 30 min sonication to form a brownish dispersion of GO with a concentration of ≈0.5 mg mL^{-1}. After that, 500 mg PVA was added to GO dispersion with rigorous stirring. The GO dispersion with PVA was then moved to a round bottomed flask and placed into an oil bath. 1.2 gm of L-ascorbic acid and sufficient amount of NH$_3$ was added to the dispersed solution to maintain the pH level from 9 to 10 while maintaining a rigorous stirring. The mixed solution was kept in a closed chamber and heated at 90 °C for 24 h so that the mixture became black in color. To obtain the dispersion volume of 200 mL, DI water was added to this dispersion. The resulted rGO was then thoroughly washed to remove the residues and finally dispersed into DI water to obtain required concentrations.

Chemical Treatment and Graphene Materials Coating: Chemical treatment (alkali treatment) was used to improve the surface properties of jute fiber. Untreated jute fibers of 30 cm length were prepared, thoroughly washed with DI water, and dried in an oven at 80 °C to achieve a constant weight. Hot water treatment is one of the effective ways of removing non-cellulosic materials. Therefore, the washed and dried fiber was treated with warm water at 60 °C for 60 min, and then at 100 °C for 30 min (Figure S9c, Supporting Information). In this way, fiber weight was reduced by 6 wt% in comparison to untreated fiber. This cleaned fiber was then treated with 0.5% NaOH solution, with a material to liquor ratio (M:L) of 1:50. Alkali treatment together with hot water treatment further reduced 6 wt% of the fiber. Alkali was used to dissolve the hemicellulose, and this treated fiber was labeled as HA0.5.

A simple dip coating technique was used to coat the alkali-treated jute fiber with rGO. An optimized time of 30 min with M:L of 1:10 was used in this coating technique to create stable and uniform surface coating (Figure S11a, Supporting Information). The coated fibers were subsequently dried in the oven for 30 min at 80 °C. A range of rGO concentrations (0.25, 0.5, 0.75, 1, and 5 wt%) was used to prepare rGO-coated samples, which were labeled as rGO 0.25, rGO 0.5, rGO 0.75, rGO 1, and rGO 5, respectively.

Manufacturing of rGO-Coated Jute Fiber Preforms: The development of rGO-coated jute fiber preforms comprised of several steps which include the combination of physical, chemical, and mechanical actions. A highly aligned unidirectional preform with improved fiber packing of elementary jute fiber was prepared by following the previous study.[21] In such technique, the single elementary fiber was separated via hand combing of HA treated jute fiber, where heat and alkali treatment ensures nearly 100% single fiber separation (Figure S10a–d, Supporting Information). The alignment of such highly individualized fibers was maintained by putting a both-sided tape at both ends of the tow (Figure S10d, Supporting Information). They were then dipped into GO dispersions 30 min with M:L of 1:10 (Figure S11a,b, Supporting Information). After that, rGO-coated fibers were then hand sprayed with epoxy compatible water-based sizing materials to confirm a dry non-woven structure before hot press treatment (Figure S11c, Supporting information). Finally, the coated fibers were hot press at 1 ton inch^{-2} pressure at elevated temperature of 120 °C for 30 min (Figure S12a,b, Supporting Information). Preforms with untreated fiber were labeled as UT, heat alkali-treated jute fiber after individualization and compaction as HA0.5, and rGO treated jute fiber preform with 0.25, 0.5, 0.75, 1, and 5 mg mL^{-1} as rGO 0.25, rGO 0.5, rGO 0.75, rGO 1, and rGO 5, respectively.

Manufacturing of Composites: A vacuum assisted resin infusion process (VARI) was used to manufacture rGO-coated composites (Figure S12c, Supporting Information). A room temperature cured EL2 laminating resin and AT30 amine hardener were used in the VARI process. UD jute fiber preforms were dried in an oven at 50 °C for 5 h to ensure there was no moisture left in the fibers. Four layers of dried UD preforms were placed on a metal plate, which was previously cleaned with acetone and sprayed with PVA release agent on its surface. A peel ply was used on the bottom and top side of the preform to ensure easy de-molding of composites. In addition, a mesh fabric was also placed on top to ensure even flow of resin during the infusion process. Finally, such arrangement was fully sealed with nylon plastic bag to ensure negative atmospheric pressure inside the bag upon pumping. Resin and hardener were separately de-gassed for 30 min in a degassing chamber of vacuum pump, and after that they were mixed and again de-gassed for 15 min to ensure there were no bubbles inside the resin. The pump was then ran and ensured the bag was air-tight with no leakage. Finally, the resin was infused inside the bag by using inlet pipe and maintained a constant flow of 1 mm s^{-1}. Infused preforms were kept for 24 h inside the bag at room temperature to ensure full curing of composites (Figure S12e,f, Supporting Information).

Characterization: A digital optical microscope (Keyence VHX-500F, UK) was used to quantitatively measure the diameter of fibers, microdroplet lengths of fiber/epoxy micro-composites, and cross-sectional image of composites to observe fiber packing. Surface topography of untreated and graphene treated jute fibers were analyzed by using a Philip XL30 field emission gun SEM. Kratos axis XPS system and FTIR were used to conduct the surface characterization of untreated and treated jute fibers. Flake thicknesses were measured with a Dimension Icon (Bruker) atomic force microscope. Raman spectra of graphene flakes were collected by using a Renishaw Raman system equipped with a 633 nm laser. A TA instrument (TGA Q5000, UK) was used to study the thermal decomposition behavior of untreated and treated jute fibers from room temperature to 1000 °C in a nitrogen atmosphere at a constant heating rate of 10 °C min^{-1}.

Tensile Testing of Elementary Fibers: ASTM D3822-01 standard was followed to conduct the single fiber tensile test. Single elementary fibers (40–50 mm in length) were manually separated from the fiber bundles.

**ADVANCED
SCIENCE NEWS**

www.advancedsciencenews.com

**ADVANCED
SUSTAINABLE
SYSTEMS**

www.advsustainsys.com

Single jute fiber was then placed and glued in a paper card frame (Figure 2a), and left for 24 h to ensure the full curing of the glue. Before tensile testing, the diameter of the fiber was measured by horizontally placing them under the digital microscope. A total of five different places were selected to determine the average diameter of the fiber. As prepared samples were kept in a standard laboratory atmosphere (≈55% RH and ≈20 ± 2 °C) for at least 24 h. The tensile test of single fibers was conducted on a Zwick-Roell tensile testing machine (Zwick/Roell, UK) with a load cell of 20 N (Figure S13a, Supporting Information). A 20 mm gauge length and 2 mm min^{-1} crosshead speed were selected as per ASTM D3822-01 standard. Young's modulus of the fibers was calculated from the slope of the stress–strain curve at 0.1–0.3% strain.

Single Fiber Micro-Bond Test: A micro-bond test was carried out to measure the IFSS by following the previously reported work (Figure 2h).[20] Fiber and paper frame were prepared by following the similar method as single fiber tensile test. In order to prepare micro-droplet of resin on a single jute fiber, a single glass fiber strand was used. The tip of the glass fiber was dipped into the previously mixed resin and hardener. A micro-droplet of resin was stuck on the tip of the glass fiber, and then carefully mounted on the jute single fiber. Two droplets were placed in a single paper frame and left it overnight to cure the resin with jute fiber. A digital microscope was used to measure the diameter and embedded microdroplet length of the resin on jute fiber. A microvice, with one-sided rotating shaft with two sharp blades, was used to conduct the micro-bond test (Figure S13b, Supporting Information). A Zwick-Roell tensile testing machine (UK) was used with 20 N load cell and a crosshead speed of 0.25 mm min^{-1}. 30 samples were tested for each set and calculated the average IFSS. It was assumed that the force generated during test to de-bond the interface of jute fiber and matrix was uniformly developed and therefore, the following Equation (1) could be used to calculate the IFSS.

$$\tau_{IFFS} = \frac{F}{\pi D l_e} \tag{1}$$

where, τ_{IFFS} is the IFSS, F is the maximum pull-out force, l_e is embedded droplet length and D is the fibre diameter.

Mechanical Testing of the Composites: ASTM D3039 standard was followed to carry out the longitudinal and transverse tensile test of untreated and rGO-coated jute fiber/epoxy composites. A total of five specimens (size: 250 mm × 15 mm) were prepared for testing each type of composites. Glass fiber tabbing was used on each sample to ensure even stress development and avoid any premature failure. An Instron 5985 tensile testing machine (UK) was used, which was equipped with 100 kN load cell and a video extensometer to record the extension of materials (Figure S13c,d, Supporting Information). The crosshead speed was kept 2 mm min^{-1} for this test. Young's modulus, tensile strength, and failure strain for each sample were collected from the machine exported datasheet.

Electro-Magnetic Interference Shielding Tests: A Vector network analyzer (HP E8363B, Agilent Technologies, Inc., Santa Clara, CA, USA) was used to measure the EMI SE with both amplitude and phase properties at a frequency 8–12 GHz. The testing samples were cut to have the width of 22.9 mm, the length of 10.2 mm, and the thickness of 2 mm before the measurement. All four S-parameters were obtained and recorded. However only the S_{11} (reflected) and S_{21} (transmitted) were used to calculate the EMI SE (%) and EMI absorption of based on following equations:

$$EMI\,SE\,(\%) = (1 - S_{21}) \times 100 \tag{2}$$

$$EMI\,Absorption\,(\%) = (1 - S_{21} - S_{11}) \times 100 \tag{3}$$

Supporting Information

Supporting Information is available from the Wiley Online Library or from the author.

Conflict of Interest

The authors declare no conflict of interest.

Authors Contributions

N.K. conceived, planned, and designed the study. F.S. prepared graphene-coated jute fibers under N. K's guidance. F.S. developed, prepared and characterised jute fibre composites, and performed measurements, and data analysis for those samples under P.P's supervision. S.A. developed, prepared, and characterized rGO and graphene dispersions, and performed XPS analysis of rGO and graphene-coated jute fibers under supervision of K.S.N. and N.K. EMI shielding measurements were carried out and analyzed by M.Z. and N.K., respectively. N.K. performed analysis and discussed on sustainability and environmental impacts. N.K. wrote the manuscript with inputs from F.S., S.A., K.S.N., P.P., and M.Z. The supporting information was prepared by F.S. with inputs from N.K. All authors reviewed and approved the manuscript.

[1] Y. Zong, T. Zheng, P. Martins, S. Lanceros-Mendez, Z. Yue, M. J. Higgins, *Nat. Commun.* **2017**, *8*, 38.

[2] M. N. Karim, S. Afroj, M. Rigout, S. G. Yeates, C. Carr, *J. Mater. Sci.* **2015**, *50*, 4576.

[3] M. N. Karim, M. Rigout, S. G. Yeates, C. Carr, *Dyes Pigm.* **2014**, *103*, 168.

[4] M. Wright, A. Kirk, M. Molloy, E. Mills, *The Telegraph*, January 10, **2018**.

[5] J. Zheng, S. Suh, *Nat. Clim. Change* **2019**, *9*, 374.

[6] M. Barth, M. Carus, http://eiha.org/media/2017/01/15-04-Carbon-Footprint-of-Natural-Fibres-nova1.pdf (accessed: September 2017).

[7] U. G. K. Wegst, H. Bai, E. Saiz, A. P. Tomsia, R. O. Ritchie, *Nat. Mater.* **2015**, *14*, 23.

[8] M. Alkbir, S. Sapuan, A. Nuraini, M. Ishak, *Compos. Struct.* **2016**, *148*, 59.

[9] G. Koronis, A. Silva, M. Fontul, *Composites, Part B* **2013**, *44*, 120.

[10] J. Gassan, A. K. Bledzki, *Compos. Sci. Technol.* **1999**, *59*, 1303.

[11] M. Sen, R. Mukherjee, *J. Text. Inst., Proc.* **1952**, *43*, P114.

[12] R. H. Baughman, C. Cui, A. A. Zakhidov, Z. Iqbal, J. N. Barisci, G. M. Spinks, G. G. Wallace, A. Mazzoldi, D. De Rossi, A. G. Rinzler, *Science* **1999**, *284*, 1340.

[13] N. Karim, M. Zhang, S. Afroj, V. Koncherry, P. Potluri, K. S. Novoselov, *RSC Adv.* **2018**, *8*, 16815.

[14] S. V. Ahir, E. M. Terentjev, *Nat. Mater.* **2005**, *4*, 491.

[15] X. Yu, H. Cheng, M. Zhang, Y. Zhao, L. Qu, G. Shi, *Nat. Rev. Mater.* **2017**, *2*, 17046.

[16] M. F. De Volder, S. H. Tawfick, R. H. Baughman, A. J. Hart, *Science* **2013**, *339*, 535.

[17] S. Afroj, S. Tan, A. M. Abdelkader, K. S. Novoselov, N. Karim, *Adv. Funct. Mater.* **2020**, *30*, 2000293.

[18] A. K. Geim, K. S. Novoselov, *Nat. Mater.* **2007**, *6*, 183.

[19] K. S. Novoselov, A. K. Geim, S. V. Morozov, D. Jiang, Y. Zhang, S. V. Dubonos, I. V. Grigorieva, A. A. Firsov, *Science* **2004**, *306*, 666.

[20] F. Sarker, N. Karim, S. Afroj, V. Koncherry, K. S. Novoselov, P. Potluri, *ACS Appl. Mater. Interfaces* **2018**, *10*, 34502.

[21] F. Sarker, P. Potluri, S. Afroj, V. Koncherry, K. S. Novoselov, N. Karim, *ACS Appl. Mater. Interfaces* **2019**, *11*, 21166.

[22] A. M. Abdelkader, N. Karim, C. Vallés, S. Afroj, K. S. Novoselov, S. G. Yeates, *2D Mater.* **2017**, *4*, 035016.

[23] S. Afroj, N. Karim, Z. Wang, S. Tan, P. He, M. Holwill, D. Ghazaryan, A. Fernando, K. S. Novoselov, *ACS Nano* **2019**, *13*, 3847.

[24] S. Pei, H.-M. Cheng, *Carbon* **2012**, *50*, 3210.

[25] N. Karim, S. Afroj, S. Tan, P. He, A. Fernando, C. Carr, K. S. Novoselov, *ACS Nano* **2017**, *11*, 12266.

[26] N. Karim, S. Afroj, A. Malandraki, S. Butterworth, C. Beach, M. Rigout, K. S. Novoselov, A. J. Casson, S. G. Yeates, *J. Mater. Chem. C* **2017**, *5*, 11640.

[27] A. M. Abdelkader, D. J. Fray, *Nanoscale* **2017**, *9*, 14548.

[28] M. S. Zoromba, M. H. Abdel-Aziz, M. Bassyouni, S. Gutub, D. Demko, A. Abdelkader, *ACS Sustainable Chem. Eng.* **2017**, *5*, 4573.

[29] L. Y. Mwaikambo, M. P. Ansell, *J. Appl. Polym. Sci.* **2002**, *84*, 2222.

[30] K. T. Faber, A. G. Evans, *Acta Metall.* **1983**, *31*, 565.

[31] Z. Xu, H. Sun, X. Zhao, C. Gao, *Adv. Mater.* **2013**, *25*, 188.

[32] R. Wang, J. Sun, L. Gao, C. Xu, J. Zhang, *Chem. Commun.* **2011**, *47*, 8650.

[33] M. Tian, L. Qu, X. Zhang, K. Zhang, S. Zhu, X. Guo, G. Han, X. Tang, Y. Sun, *Carbohydr. Polym.* **2014**, *111*, 456.

[34] J. Chen, D. Zhao, X. Jin, C. Wang, D. Wang, H. Ge, *Compos. Sci. Technol.* **2014**, *97*, 41.

[35] B. Madsen, A. Thygesen, H. Lilholt, *Compos. Sci. Technol.* **2009**, *69*, 1057.

[36] L. Y. Mwaikambo, *BioResources* **2009**, *4*, 566.

[37] R.-C. Zhuang, T. T. L. Doan, J.-W. Liu, J. Zhang, S.-L. Gao, E. Mäder, *Carbon* **2011**, *49*, 2683.

[38] A. Hamdan, M. T. H. Sultan, F. Mustapha, in *Structural Health Monitoring of Biocomposites, Fibre-Reinforced Composites and Hybrid Composites* (Eds: M. Jawaid, M. Thariq, N. Saba), Woodhead Publishing, Cambridge, UK **2019**, pp. 227–242.

[39] C. Xia, J. Yu, S. Q. Shi, Y. Qiu, L. Cai, H. F. Wu, H. Ren, X. Nie, H. Zhang, *Composites, Part B* **2017**, *114*, 121.

[40] C. Xia, H. Ren, S. Q. Shi, H. Zhang, J. Cheng, L. Cai, K. Chen, H.-S. Tan, *Appl. Surf. Sci.* **2016**, *362*, 335.

[41] C. Blackman, J. Blanchard, S. Benane, D. House, *FASEB J.* **1995**, *9*, 547.

[42] N. Karim, S. Afroj, K. Lloyd, L. Clarke Oaten, D. V. Andreeva, C. Carr, A. D. Farmery, I.-D. Kim, K. S. Novoselov, *ACS Nano* **2020**, *14*, 12313.

[43] *Life Cycle Assessment of Cotton Fiber and Fabric*, Full Report, Cotton Incorporated, Cary, NC **2012**.

[44] S. S. Muthu, *Handbook of Sustainable Apparel Production*, CRC Press, Boca Raton, FL **2015**.

[45] Sustainable Apparel Coalition. The Higg Index 2.0. Available online: http://www.apparelcoalition.org/higgindex/ (accessed: August 2020).

[46] Y. Chang, T. Sun, C. Fan, X. Zhou, *Starch Nanocrystals. Compos. Interfaces* **2018**, *25*, 981.

[47] M. N. K. Chowdhury, M. D. H. Beg, M. R. Khan, M. F. Mina, *Cellulose* **2013**, *20*, 1477.

[48] H. Wang, G. Xian, H. Li, *Part A Appl. Sci. Manuf.* **2015**, *76*, 172.

[49] K.-Y. Lee, S. R. Shamsuddin, M. Fortea-Verdejo, A. Bismarck, *J. Vis. Exp.* **2014**, https://doi.org/10.3791/51432.

[50] X. Zhang, X. Fan, C. Yan, H. Li, Y. Zhu, X. Li, L. Yu, *ACS Appl. Mater. Interfaces* **2012**, *4*, 1543.

[51] W. S. Hummers, R. E. Offeman, *J. Am. Chem. Soc.* **1958**, *80*, 1339.

2000228 (12 of 12)